14-Diffraction Physics and Optics

8,9,10,12-tetrafluoro-*o*-carborane) and metallacarboranes CpFe(dicarb) and CpCo(dicarb) (Cp=C_5H_5, dicarb=dicarbollide) proving the absence of electron density accumulation inside the carborane cage and multicenter bonding at the triangular faces of the icosahedron. Among the organometallic compounds the metallocene derivatives Cp_2V, CpFeCp* (Cp*=C_5Me_5) and CpTi(η^8-C_8H_8) were studied. On the contrary to the disordered ferrocene, the structures of Cp_2V and CpFeCp* are ordered at low temperature and the asymmetry of the *3d*-electron distribution around metal atoms and the nature of metal-ligand bonds were analyzed. The observed EDD's in the molecules studied are essential for analysis of chemical bond features.

PS-14.02.11 ELECTRON DENSITY DISTRIBUTION IN THE NITROGEN-CONTAINING HETEROCYCLES. By *E.A.Kuz'mina, M.Yu.Antipin* and Yu.T.Struchkov.* A.N.Nesmeyanov Institute of Organoelement Compounds, Russian Academy of Sciences, Moscow, Russian Federation.

Using high-resolution (sin $\theta/\lambda \leq 1.0$ Å^{-1}) low temperature (120-140 K) X-ray diffraction data electron density distribution analysis in the new nitrogen-containing heterocycles (I-III) was performed in order to elucidate essential features of the chemical bonding.

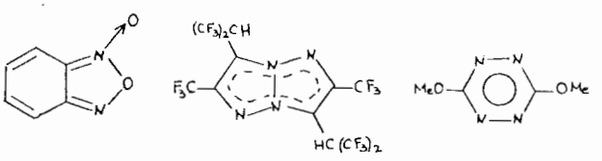

A conventional high-angle (R=3.0-4.0%) and multipole refinement (MOLLY program) procedures were used for constructing the dynamic and static deformation electron density (DED) maps, calculation of atomic charges and multipole parameters (final R values after multipole refinement were in the range of 1.9-2.4%). For the benzofuroxane molecule (I) atomic charges were found to be small, positive DED peaks were localized nearly at the mid-points of the chemical bonds except for dative N→O bond,where the corresponding maximum was shifted to the O atom. An essential delocalization of the electron density in the π-region was found in this heterocycle. In the fluorinated tetraazapentalene (II) and tetrazine derivative (III) the strong π-component on the C-C, N-N and C-N bonds in the rings was established, testifying to the aromatic character of these heterocycles. Atomic charge distribution in (II) based on the multipole refinement data allowed to determine the contribution of the different resonance forms in the electronic structure. In the tetrazine derivative (III) high maxima on the DED maps corresponding to the lone pairs were found near N atoms in the molecular plane. The DED peaks on the C-N and N-N bonds were found to be shifted towards the centre of the heterocycle (bent bonds) probably due to the electrostatic repulsion between lone pairs and chemical bond electron density.

PS-14.02.12 ELECTRON DENSITY DISTRIBUTION IN CASSITERITE SnO_2. By V.S.Urusov*, O.V.Yakubovich and N.N.Eremin, Moscow State University, Russia.

The precise X-ray investigation, including δρ maps calculation was carried out to study peculiarities of chemical bonds in crystals of cassiterite SnO_2 grown by oxidation of metallic tin: a=4.739(1), c=3.1877(9) A, sp.gr. $P4_2/mnm$, Z=2, ρ_c=6.99 g/cm^3, μr=0.9, λ MoKα, 2θ-θ scanning, sin $\theta/\lambda \leq 1.08$ A^{-1}, 141 independent reflections. Parameters of the high-angle (sin $\theta/\lambda \geq 0.6$ A^{-1}, 104 refl.) refinement are: R=0.0062, wR=0.0072, s=1.1777.
The deformation electron density (δρ) maps for characteristic sections show main features common with δρ maps of isostructural rutile TiO_2 (R.Restory,D.Schwarzenbach and J.R.Schneider, Acta Cryst. (1987), B43, 251-257) and stishovite SiO_2 (M.A.Spackman, R.J.Hill and G.V.Gibbs, Phys.Chem.Min. (1987), 14,139-150). However, there are some peculiarities due to a more polarizable electron shell of Sn^{4+} compared to Ti^{4+} or Si^{4+} ions.

PS-14.02.13 SECOND-NEAREST-NEIGHBOUR INTERACTIONS AND THE ELECTRON DENSITY DISTRIBUTION IN Y_2BaCuO_5
By J. Hester, R. Hsu* and E. N. Maslen, Crystallography Centre, University of Western Australia, Nedlands, WA 6009, Australia
N. Ishizawa, Research Lab. of Engineering Materials, Tokyo Institute of Technology, 4259 Nagatsuta, Midori-Ku, Yokohama 227, Japan

Y_2BaCuO_5 has a tightly packed structure with all cations and the O3 anion coplanar in a mirror plane with *y*/*b* = 0.25. There are O1 and O2 atom pairs above and below that plane. Analysis of synchrotron data for a small Y_2BaCuO_5 crystal shows that second nearest neighbour interactions dominate the redistribution of electron density. Within the mirror plane the cations are aligned in the sequence Ba—Y2—Cu—Y1—Ba over a total length of 13.10 Å. Atoms in those lines are cross-linked by zigzag connections along the *a* axis. The difference electron density Δρ in the *y*/*b* = 0.25 plane displayed in the Figure shows that electron density is strongly depleted along the shorter links in that grid.

14-Diffraction Physics and Optics

382

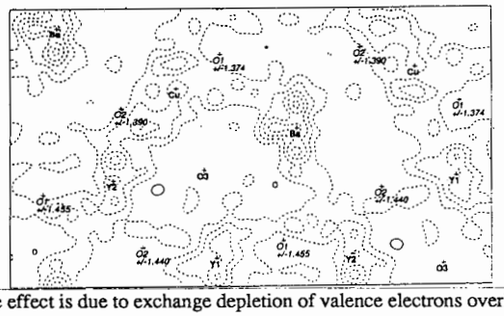

The effect is due to exchange depletion of valence electrons overlapping with closed electron sub-shells. The Δρ sections perpendicular to the $y/b = 0.25$ plane show relocation of density from within to above and below that plane. Atomic charges, determined by projecting Δρ onto atomic density basis functions (F L Hirshfeld, Isr. J. Chem, 1977, 16, 198-201) are 2.8(1), 2.1(1), 1.6(1), 2.4(1), -1.8(1), -1.8(1), and -1.8(1) for Y1, Y2, Ba, Cu, O1, O2 and O3 respectively. The O atom charges are far more consistent than values determined earlier with Mo $K\alpha$ radiation. Those charges reflect partial transfer of valence electron density from cation to anion by exchange depletion.

The distances from each cation to the nearest neighbour O atoms are Y1 2.275(2)—2.379(1), Y2 2.302—2.355(1), Ba 2.611(2)—3.248(1) and Cu 1.974(1)—2.208(2) Å. Mean values are Y1—O 2.34(2), Y2—O 2.33(1), Ba—O 2.87(5) and Cu—O 2.04(6) Å. The topography of the deformation density can be understood only in terms of cation radii larger than those of the oxygen anions. Values of 1.79, 1.98, 1.34 and 1.16 Å for Y, Ba, Cu and O respectively used in the modelling the structure imply that the structural architecture for Y_2BaCuO_5 is determined by second-nearest-neighbour cation—cation interactions rather than anion—anion or cation—anion interactions. That model is supported by the vibration tensors, which are compact along the shorter cation-cation vectors, but extend along the anion-anion vectors. If exchange interactions are involved in the mechanism for high temperature superconductivity in the closely related $YBa_2Cu_3O_{7-\delta}$, it may be advisable to consider interactions beyond the first coordination sphere.

PS-14.02.14 DEFORMATION DENSITIES IN SIMPLE RARE EARTH COMPOUNDS By B. E. Eschtmann, E. N. Maslen, and N. R. Streltsova* *Crystallography Centre, University of Western Australia, Nedlands, 6009, Australia*

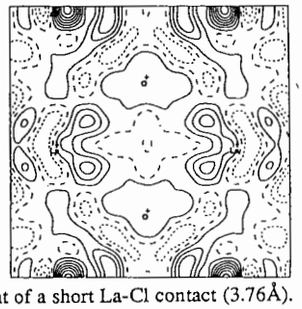

The deformation density Δρ for LaOCl was determined for a naturally-faced single crystal measured with Mo $K\alpha$ radiation. The La coordination may be described as a mono-capped square antiprism. Neighbouring La atoms are connected by the oxygen double bridge shown (La-La 3.78Å).

There are Δρ peaks at the mid-point of a short La-Cl contact (3.76Å).

Δρ maps evaluated with extinction corrections that minimize differences between equivalent reflection intensities are closely approximated by those which optimize an extinction parameter as part of the least squares structure refinement.

Space group $P4/nmm$, tetragonal, M_r = 190.36, a = 4.1218 (8) Å, c = 6.888 (1) Å, V = 117.03 (6) Å^3, Z = 2, D_x = 5.402 Mg m^{-3}, μMo $K\alpha$ = 18.99 mm^{-1}, $F(000)$ = 164, T = 293 K, R = 0.014, wR = 0.013, S = 1.87 for 126 unique reflections.

Deformation densities for rare earth oxides and oxy-halides currently being studied with Mo $K\alpha$ (λ = 0.71073 Å) and with synchrotron radiation will be described.

PS-14.02.15 X-RAY STUDY OF THE ELECTRON DENSITY IN RHOMBOHEDRAL CARBONATES: $CaCO_3$, $MgCO_3$, $MnCO_3$. By E. N. Maslen, V. A. Streltsov* and N. R. Streltsova, Crystallography Centre, University of Western Australia, Australia.

Calcite, $CaCO_3$, is an abundant carbonate mineral. Its structure is isomorphous with that of several carbonate mineral constituents of sedimentary rocks, including magnesium- and transition metal-bearing carbonates. The calcite structure has the same space group, $R\bar{3}c$, as another widely distributed mineral, corundum (α-Al_2O_3), a benchmark compound for which the electron density has been measured several times over the past decade. A sketch of the calcite structure coordination close to the cations is shown in Fig.1. The deformation electron density (Δρ) in naturally-faced single crystals of synthetic $CaCO_3$ and the minerals: magnesite, $MgCO_3$, and rhodochrosite, $MnCO_3$, was determined using diffraction data measured with Mo $K\alpha$ (λ = 0.71073 Å) and 0.7Å synchrotron X-radiation. A specimen of $CaCO_3$ grown directly from aqueous solution was bounded by two {104}, two {$\bar{1}$14}, two {0$\bar{1}$4} and one {1$\bar{2}$3} faces with dimensions 31x36x46x37μm respectively from the crystal centre. Cleavage fragments of $MgCO_3$ and $MnCO_3$ mineral rocks were bounded by the same first six faces with dimensions 24x55x77μm and 40x24x49μm respectively from the crystal centres. Sets of structure factors for synchrotron radiation and Mo $K\alpha$ tube radiation for these crystals are consistent. Extinction corrections that minimize differences between equivalent reflection intensities (Maslen and Spadaccini, *Acta Cryst.*, 1993, in press) have been applied. This correction (y_{min}=0.80) for $CaCO_3$ is closely approximated by the values which optimize the extinction parameter as part of the least squares structure refinement. The extinction effect for $MgCO_3$ was small (y_{min}=0.96). No extinction was observed for $MnCO_3$. A map of Δρ through the CO_3 group in the (0001) plane for $CaCO_3$ from X-ray tube data is shown in Fig.2. The general topographies of the Δρ maps are broadly similar for all the carbonates studied. There are 0.26eÅ^{-3} high density maxima in the C-O bonds and 0.28eÅ^{-3} maxima at the O-atom lone pairs. Corresponding values of Δρ for $MgCO_3$ and $MnCO_3$ are 0.58eÅ^{-3} and 0.80eÅ^{-3} in the C-O bonds, and 0.40eÅ^{-3} and 0.50eÅ^{-3} at the O-atom lone pairs. The maxima in the Δρ maps for $CaCO_3$ are lower than those for $MgCO_3$ and $MnCO_3$. This can be attributed to greater exchange depletion when the more diffuse radial electron distribution of the Ca cation overlaps with the CO_3 group. Aspherical charge destribution around the d-metal Mn can be related to the octahedral crystal field. Atomic charges determined by projecting Δρ onto atomic density basis functions (Hirshfeld, 1977, *Isr. J. Chem.*, 16, 198-201) are Ca +0.16(2)e, C +0.23(2)e and O -0.13(1)e for $CaCO_3$, and Mg +0.06(2)e, C +0.21(2)e and O -0.09(1)e for $MgCO_3$ and Mn +0.43(5)e, C +0.17(4)e and O -0.20(1)e for $MnCO_3$.

X-ray tube data at T=293K, Space group $R\bar{3}c$, hexagonal, Z=6: $CaCO_3$, M_r=100.09, a=4.991(2)Å, c=17.062(2)Å, V=368.1(3)Å^3, D_x= 2.709Mg/m^3, μ$_{MoK\alpha}$=2.134mm^{-1}, $F(000)$=300, R=0.017, wR=0.023, S=4.52, 328 unique reflections; $MgCO_3$, M_r=84.31, a=4.635(1)Å, c=15.023(2)Å, V=279.5(1)Å^3, D_x=3.005Mg/m^3, μ$_{MoK\alpha}$=0.59mm^{-1}, $F(000)$=252, R =0.022, wR=0.027, S=6.59, 332 unique reflections; $MnCO_3$, M_r=114.95, a=4.773(1)Å, c= 5.642(1)Å, V=308.6(1)Å^3, D_x=3.711Mg/m^3, μ$_{MoK\alpha}$=5.85mm^{-1}, $F(000)$=330, R=0.019, wR=0.028, S=3.23, 368 unique reflections.